Explore the effect of annealing temperature on thickness and electrical properties of Y_2O_3 thick films

Dr. Upendra Devendra Lad

Department of Physics
Mahatma Gandhi Vidya Mandir's Arts, Science and Commerce College, Manmad, Affiliated to Savitribai Phule Pune University
Pune, Maharashtra, India 423104

Abstract:
In this study, screen-printed yttrium oxide (Y_2O_3) thick films were fabricated and annealed at three different temperatures, namely 100 °C, 200 °C, and 300 °C, for 3 hours in a closed muffle furnace to investigate the influence of annealing temperature on their thickness and electrical properties. The film thickness was measured using the mass difference method, while electrical resistivity was evaluated by the half-bridge technique. The results revealed that both thickness and resistivity of the films decreased with increasing annealing temperature, indicating enhanced densification and improved charge transport. The thickness of the films was found to reduce from 26 µm to 18 µm as the annealing temperature increased, while the resistivity decreased from 169435.2 Ω·m at 100 °C to 93013.4 Ω·m at 300 °C. The temperature coefficient of resistance (TCR) was also calculated and found to be -0.00343, -0.00217, and -0.00208 /°C for films annealed at 100, 200, and 300 °C, respectively, demonstrating a negative TCR characteristic. These findings confirm that annealing temperature has a significant impact on the structural densification and electrical performance of Y_2O_3 thick films, making it a crucial parameter for optimizing their functional properties for electronic applications.

Keywords: Screen-printed, annealing temperature, thickness, resistivity, TCR.

1. INTRODUCTION

Recent advancements in metal oxides have greatly expanded their role in energy, catalysis, sensing, electronics, and biomedical applications due to their tunable structural, electrical, and optical properties [1, 2]. In energy storage, oxides such as MnO_2, Co_3O_4, NiO, and mixed systems are widely used in supercapacitors and batteries for their high capacitance and redox activity, with binary/ternary oxides and doped nanostructures showing improved stability and performance. In catalysis and photocatalysis, TiO_2, ZnO, CeO_2, and WO_3 are applied in water splitting, CO_2 reduction, and pollutant degradation, with recent progress in bandgap engineering, surface modification, and coupling with graphene materials enhancing their activity [3, 4]. For gas sensing, nanostructured SnO_2, In_2O_3, and Fe_2O_3 exhibit excellent sensitivity, selectivity, and fast response times, aided by morphology control and noble metal functionalization. In electronics, high-κ dielectric oxides such as HfO_2, Y_2O_3, and Al_2O_3 are key in advanced transistors, memory devices, and insulating layers, while transparent conducting oxides like ITO and doped ZnO are crucial in solar cells, displays, and LEDs [4-6]. Biocompatible oxides including TiO_2 and ZrO_2 are applied in implants, drug delivery, and antibacterial coatings. The Y_2O_3 has gained attention for its excellent thermal stability, wide bandgap, and high dielectric constant, making it useful in gate dielectrics, protective coatings, and sensing applications [6-8].

Annealing temperature plays a vital role in tuning the structural, morphological, optical, and electrical properties of metal oxide materials, which directly impacts their performance in applications such as sensors, catalysts, dielectrics, supercapacitors, and photocatalysts [9, 10]. At low temperatures, films often remain amorphous, porous, and resistive due to residual organics and defects, while higher annealing promotes crystallinity, grain growth, and densification, thereby reducing thickness, enhancing conductivity, and

improving stability. For example, TiO_2 and ZnO show improved phase purity and optical properties with proper annealing, while Y_2O_3 thick films exhibit reduced resistivity and better grain connectivity [8-10]. However, excessive annealing can lead to abnormal grain growth, cracking, or loss of oxygen vacancies, which may degrade electrical performance. Optimized annealing also enhances device-specific properties such as gas sensitivity in SnO_2 sensors, dielectric constant in Y_2O_3 films, optical transmittance in ITO, and photocatalytic efficiency in TiO_2 and CeO_2. The annealing temperature must be carefully controlled to balance densification, crystallinity, porosity, and defect chemistry, thereby ensuring high performance, stability, and reliability of metal oxide–based materials across diverse technological applications [10, 11].

Yttrium oxide (Y_2O_3) nanoparticles are an important class of rare-earth metal oxide nanomaterials that have attracted significant attention due to their unique structural, electrical, optical, and thermal properties, which make them suitable for a wide range of advanced technological applications [12, 13]. Y_2O_3 crystallizes in a cubic bixbyite structure and possesses a wide bandgap of about 5.5–5.8 eV, excellent thermal stability, and chemical inertness, which distinguish it from many other oxides. At the nanoscale, Y_2O_3 exhibits a high surface-to-volume ratio, tunable particle size, and controllable morphology, which enhance its reactivity and functional properties compared to bulk material. Several synthesis methods such as sol–gel, co-precipitation, hydrothermal, combustion, and thermal decomposition have been reported to prepare Y_2O_3 nanoparticles with uniform size distribution and controlled crystallinity. Their small particle size and high surface activity enable novel applications in optoelectronics, catalysis, sensing, and biomedical fields. Due to their high dielectric constant and low leakage current, Y_2O_3 nanoparticles are employed as high-κ gate dielectrics in microelectronics [14, 15]. Their thermal stability and chemical resistance also allow their use as protective coatings, refractory materials, and laser ceramics. In the biomedical domain, Y_2O_3 nanoparticles are being explored for drug delivery, bioimaging, and radiation therapy owing to their biocompatibility and unique luminescence properties when doped with rare-earth elements [15, 16]. Y_2O_3 nanoparticles have shown promise in photocatalysis and environmental remediation because of their ability to support charge transfer and surface reactions. Overall, the nanoscale engineering of Y_2O_3 not only enhances its intrinsic physical and chemical characteristics but also expands its utility in emerging fields such as energy storage, nanophotonics, and healthcare technologies [17].

The aim of the present work is to investigate the influence of annealing temperature on the thickness and electrical properties of screen-printed yttrium oxide thick films. Specifically, the study focuses on understanding how varying annealing conditions modify the film thickness, resistivity, and temperature coefficient of resistance (TCR). By establishing the correlation between annealing temperature and the functional behavior of Y_2O_3 thick films, the work aims to optimize processing parameters for their potential applications in microelectronics, sensing devices, and other advanced technologies.

2. MATERIALS AND METHODS

For the fabrication of Y_2O_3 thick films, commercially available AR-grade yttrium oxide nanoparticles were utilized due to their high purity. The films were prepared using the screen-printing technique, a versatile and widely adopted method for fabricating uniform thick films with controlled thickness and surface morphology. Glass substrates were selected as the base material owing to their smooth surface, chemical stability, and compatibility with high-temperature processing. To formulate a printable paste suitable for screen printing, a carefully optimized 70:30 ratio of inorganic to organic components was employed, where the inorganic phase consisted of Y_2O_3 nanoparticles, while the organic phase comprised a binder and solvents such as ethyl cellulose (EC) as the binder and butyl carbitol acetate (BCA) as the solvent. This ratio was chosen to achieve the required viscosity and thixotropic behavior of the paste, enabling smooth flow through the screen mesh while maintaining sufficient cohesion to prevent spreading after deposition. After the paste was prepared, it was uniformly printed onto the glass substrates using a stainless steel screen, ensuring consistent film coverage. The printed films were then dried under an infrared (IR) lamp for about 30–40 minutes to evaporate excess solvent, promote binder solidification, and prevent the formation of cracks or pinholes in the film. The dried samples were subsequently subjected to thermal annealing in a closed muffle furnace at different temperatures - 100 °C, 200 °C, and 300 °C for a duration of 3 hours. This controlled thermal treatment step was crucial for the removal of organic residues, densification of the films, and modification of their microstructural and electrical properties, thereby enabling a systematic investigation of the role of annealing temperature in tuning the properties of Y_2O_3 thick films [18, 19].

The thickness of the Y_2O_3 thick films was evaluated using the mass difference method (Eq. 1), which is a simple and effective approach to estimate the thickness of screen-printed films. In this method, the thickness is calculated from the difference in mass of the substrate before and after film deposition, considering the known density of the film material and the substrate area [19, 20].

$$\text{Thickness } (t) = M2 - M1/\rho \cdot A \qquad \text{(Eq. 1)}$$

Where,
t = thickness of the film (μm),
M2 = mass of the substrate with deposited film (g),
M1 = mass of the bare substrate before deposition (g),
ρ = density of the deposited material (g/cm³),
A = area of the deposited film (cm²).

The electrical properties of the Y_2O_3 thick films were determined using the half-bridge method, which is a widely employed technique for evaluating the resistance. The schematic diagram shown in Fig. 1 represents the half-bridge method employed for measuring the electrical properties of Y_2O_3 thick films. In this configuration, the Y_2O_3 thick film acts as one arm of the bridge, while a high precision reference resistor (Rref = 10 MΩ) is connected in series as the second arm. A regulated DC power supply of +30 V is applied across the circuit to provide the necessary bias voltage for current flow. The potential drop across the reference resistor is measured using a highly sensitive digital millivolt meter (mV) [19-21].

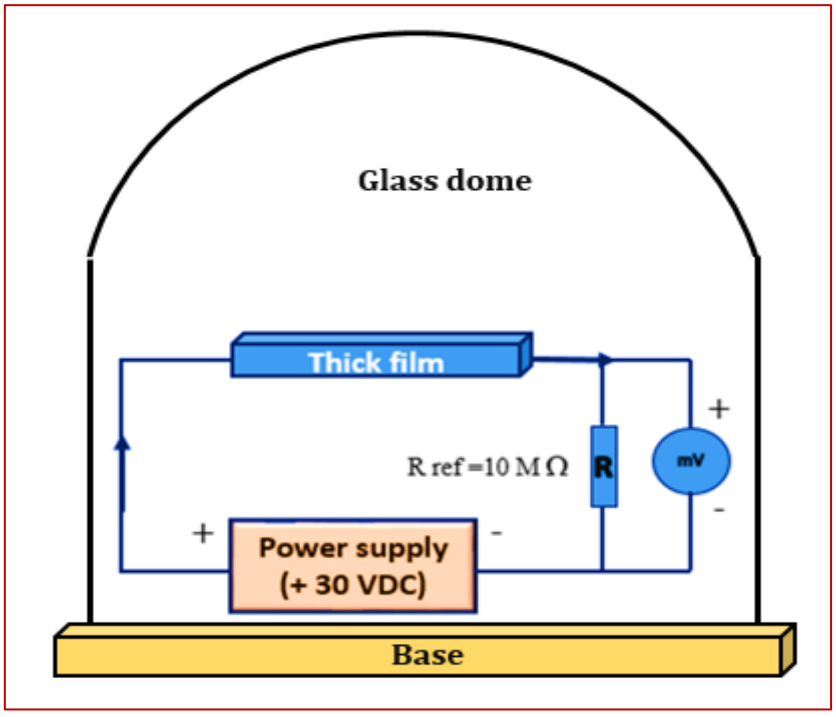

Figure 1. Schematic diagram of half bridge method

The resistivity, TCR and activation energy of Y_2O_3 thick films were estimated using Eqs. 2, 3 and 4 respectively [18-20].

$$\rho = \left(\frac{R \times b \times t}{l}\right) \Omega - m \qquad \text{(Eq. 2)}$$

Where,
ρ = Resistivity of prepared film,
R = resistance at normal temperature,
b = breadth of film,
t = thickness of the film,
l = length of the film.

$$TCR = \frac{1}{R_o}\left(\frac{\Delta R}{\Delta T}\right) \ /^{O} C \qquad \text{(Eq. 3)}$$

Where,
ΔR = change in resistance between temperature T_1 and T_2,
ΔT = temperature difference between T_1 and T_2 and
R_o = room temperature resistance of the film.

$$\Delta E = Ae^{-Ea/kBT} \quad \text{eV} \qquad \text{(Eq. 4)}$$

Where,
ΔE = Activation energy,
T = Temperature in Kelvin and
A = Arrhenius prefactor.

3. RESULT AND DISCUSSION

Figure 2(a) shows the variation of resistance with temperature for Y_2O_3 thick films annealed at 100, 200, and 300 °C. In all three cases, resistance decreases monotonically with an increase in temperature, confirming the semiconducting nature of Y_2O_3. This negative temperature coefficient of resistance arises from thermally activated conduction, where more charge carriers are excited into the conduction band as temperature rises [18, 20]. At 300 K, the film annealed at 100 °C exhibits the highest resistance (~1.3 × 10^{10} Ω), followed by the 200 °C film (~1.2 × 10^{10} Ω), while the 300 °C film shows the lowest resistance (~1.0 × 10^{10} Ω). This trend remains consistent across the entire temperature range, reflecting the systematic reduction in resistivity with increasing annealing temperature [20, 21].

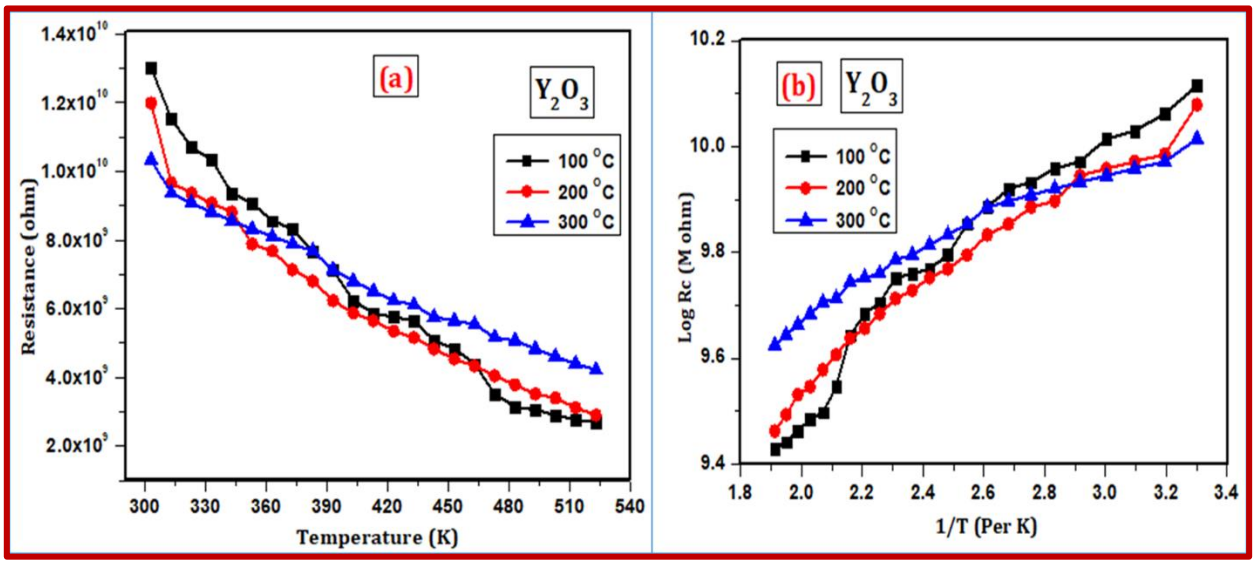

Figure 2. (a) Resistance versus temperature plot & (b) log Rc/inverse of temperature plot of Y_2O_3 thick films.

It is also observed that, at higher temperatures (above ~450 K), all samples show a more rapid fall in resistance, which is attributed to enhanced thermal activation of carriers and improved intergranular conduction. This behavior indicates that annealing improves crystallinity and particle connectivity, reducing grain boundary barriers and thereby lowering overall resistance [21, 22].

Figure 2(b) presents the Arrhenius plots, i.e., log R versus 1/T, for the Y_2O_3 thick films. The linear behavior in both high-temperature (HTR) and low-temperature (LTR) regions indicates that conduction follows thermally activated Arrhenius-type transport. The slopes of these linear regions were used to estimate the activation energy values for charge conduction. The annealed samples show distinct slopes in the LTR and HTR regions, suggesting different conduction mechanisms dominating in each regime [18, 19]. For the film annealed at 100 °C, the activation energy was 0.0639 eV in the LTR and 0.0917 eV in the HTR. For the 200 °C film, these values were 0.0291 eV (LTR) and 0.1393 eV (HTR). Similarly, the 300 °C film exhibited activation energies of 0.0288 eV (LTR) and 0.1014 eV (HTR). These values confirm that conduction is easier at lower temperatures due to shallow trap levels, whereas deeper trap levels or intrinsic conduction mechanisms dominate at higher temperatures. Interestingly, the 200 °C sample shows the highest HTR

activation energy (0.1393 eV), which may be attributed to optimized crystallization and reduced defect density at this intermediate annealing temperature.

Table 1. Electrical outcomes Y_2O_3 thick films.

Annealing Temp. (°C)	Thickness (µm)	Resistivity (Ω.m)	TCR (/°C)	Activation energy (eV)	
				HTR	LTR
100	26	169435.2	-0.00343	0.0917	0.0639
200	22	131890.1	-0.00217	0.1393	0.0291
300	18	93013.4	-0.00208	0.1014	0.0288

As shown in Table 1, the thickness of Y_2O_3 thick films decreases with increasing annealing temperature: from 26 µm at 100 °C to 22 µm at 200 °C, and further to 18 µm at 300 °C. This reduction is due to the densification and shrinkage of the film as volatile organics are removed and the microstructure becomes more compact during thermal treatment [19, 22].

The resistivity values also show a decreasing trend with annealing temperature. At 100 °C, the resistivity is 169,435.2 Ω·m, which reduces to 131,890.1 Ω·m at 200 °C and further to 93,013.4 Ω·m at 300 °C. The decrease in resistivity can be attributed to improved grain growth, increased particle-to-particle connectivity, and a reduction in grain boundary resistance. The densification of the film ensures better electron transport pathways, thereby enhancing conductivity [20, 22]. This clear inverse relationship between annealing temperature and resistivity confirms that thermal treatment is a critical step in optimizing the electrical performance of Y_2O_3 films. The TCR values, as listed in Table 1, are negative for all films, which is typical for semiconducting oxides. For the 100 °C annealed film, the TCR is –0.00343 /°C, while for the 200 °C and 300 °C annealed films, it is –0.00217 /°C and –0.00208 /°C, respectively. The magnitude of TCR decreases with increasing annealing temperature, indicating that the films become more stable and less temperature-sensitive at higher annealing temperatures. This reduction in TCR can be linked to enhanced crystallinity and reduced trap-assisted conduction after annealing [18, 23].

CONCLUSIONS

The Y_2O_3 thick films were successfully fabricated using the screen-printing technique and annealed at different temperatures to study their electrical properties. The results revealed that annealing temperature significantly influences the film thickness, resistivity, TCR, and activation energy. With increasing annealing temperature, the films exhibited a reduction in thickness and resistivity due to improved densification, grain growth, and better particle connectivity, leading to enhanced electrical conduction. All films displayed a negative temperature coefficient of resistance, confirming their semiconducting nature, while the magnitude of TCR decreased with annealing, indicating greater electrical stability. Arrhenius analysis further demonstrated thermally activated conduction mechanisms, with distinct activation energies in low- and high-temperature regions. Overall, the findings highlight that controlled annealing is an effective strategy to optimize the microstructural and electrical performance of Y_2O_3 thick films, making them promising candidates for applications in electronic, dielectric, and gas-sensing devices.

Acknowledgment

The authors sincerely thank the Principal of Mahatma Gandhi Vidyamandir's Arts, Science and Commerce College, Manmad, Tal- Nandgaon, Dist. Nasik, India, for providing the essential laboratory facilities and support to carry out the present research work.

REFERENCES:

1. Rastogi, A., Zivcak, M., Sytar, O., Kalaji, H.M., He, X., Mbarki, S. and Brestic, M., 2017. Impact of metal and metal oxide nanoparticles on plant: a critical review. *Frontiers in chemistry*, *5*, p.78.
2. Franke, M.E., Koplin, T.J. and Simon, U., 2006. Metal and metal oxide nanoparticles in chemiresistors: does the nanoscale matter?. *small*, *2*(1), pp.36-50.
3. Yu, X., Marks, T.J. and Facchetti, A., 2016. Metal oxides for optoelectronic applications. *Nature materials*, *15*(4), pp.383-396.

4. Chavali, M.S. and Nikolova, M.P., 2019. Metal oxide nanoparticles and their applications in nanotechnology. *SN applied sciences*, *1*(6), p.607.
5. Arora, A.K., Sharma, A. & Kumar, S., 2019. Electrical and dielectric properties of rare-earth oxide thick films. *Journal of Materials Science: Materials in Electronics*, 30(7), pp.6578–6586.
6. Bedi, R.K. & Singh, I., 2011. Structural, electrical and gas sensing properties of screen-printed metal oxide thick films. *Sensors and Actuators B: Chemical*, 160(1), pp.411–418.
7. Chen, X., Li, Y. & Xu, H., 2018. Advances in rare earth oxide thin and thick films: preparation, properties and applications. *Progress in Materials Science*, 97, pp.283–346.
8. Cho, Y., Park, C. & Kim, D., 2004. Temperature dependence of electrical resistivity of oxide thick films. *Journal of the European Ceramic Society*, 24(5), pp.1201–1206.
9. Akgul, F.A., Akgul, G., Yildirim, N., Unalan, H.E. and Turan, R., 2014. Influence of thermal annealing on microstructural, morphological, optical properties and surface electronic structure of copper oxide thin films. *Materials Chemistry and Physics*, *147*(3), pp.987-995.
10. Narayanan, G.N., Ganesh, R.S. and Karthigeyan, A., 2016. Effect of annealing temperature on structural, optical and electrical properties of hydrothermal assisted zinc oxide nanorods. *Thin Solid Films*, *598*, pp.39-45.
11. Muthee, D.K. and Dejene, B.F., 2021. Effect of annealing temperature on structural, optical, and photocatalytic properties of titanium dioxide nanoparticles. *Heliyon*, *7*(6).
12. Deshpande, R., Patil, D. & Mane, R., 2016. Fabrication of screen-printed Y_2O_3 thick films and their electrical characterization. *Materials Today: Proceedings*, 3(9), pp.3262–3268.
13. Rajakumar, G., Mao, L., Bao, T., Wen, W., Wang, S., Gomathi, T., Gnanasundaram, N., Rebezov, M., Shariati, M.A., Chung, I.M. and Thiruvengadam, M., 2021. Yttrium oxide nanoparticle synthesis: an overview of methods of preparation and biomedical applications. *Applied Sciences*, *11*(5), p.2172.
14. Bhavani, G. and Ganesan, S., 2016. Structural, morphological and optical study of bismuth and zinc co-doped yttrium oxide prepared by solvothermal and wet chemical method. *Acta Physica Polonica A*, *130*(6), pp.1373-1379.
15. Pazura, Y.I., Baumer, V.N., Deyneka, T.G., Vovk, O.M. and Yavetskiy, R.P., 2010. Synthesis of Y_2O_3 and Y_2O_3: Nd^{3+} monodisperse crystalline nanospheres by homogenous precipitation. *Functional Materials*.
16. Baumer, V.N., Kosmyna, M.B., Nazarenko, B.P., Puzikov, V.M., Shekhovtsov, A.N., Gordienko, L.S., Yasukevich, A.S., Kuleshov, N.V., Gulevich, A.E. and Demesh, M.P., 2012. Influence of processing conditions on the structure and properties of yttrium oxide ceramics. *Functional materials*.
17. Patil, A.S., Patil, A.V., Dighavkar, C.G., Adole, V.A. and Tupe, U.J., 2022. Synthesis techniques and applications of rare earth metal oxides semiconductors: A review. *Chemical Physics Letters*, *796*, p.139555.
18. Patil, A., Tupe, U.J. and Patil, A.V., 2021. Reduced graphene oxide screen printed thick film as NO2 gas sensor at low temperature. *Advanced Materials Research*, *1167*, pp.43-55.
19. Wagh, S.L., Tupe, U.J., Patil, A.B. and Patil, A.V., 2022. Influence of Annealing Temperature on Structural and Electrical Properties of Screen Printed Lanthanum Oxide Thick Films. *Iranian Journal of Materials Science & Engineering*, *19*(4).
20. Lad, U.D., Kokode, N.S. and Tupe, U.J., 2022. Study of pn Heterojunction Thin Films for Reducing Gas Sensing Application Fabricated by Thermal Evaporation Technique. *Advanced Materials Research*, *1172*, pp.67-82.
21. Tupe, U.J., Patil, A.V., Zambare, M.S. and Koli, P.B., 2021. Stannous Oxide Thick Film Nanosensors Design by Screen Printing Technology: Structural, Electrical Parameters and H2s Gas Detection Study. *Mater. Sci. Res. India*, *18*(1), pp.66-74.
22. Tupe, U.J., Zambare, M.S., Patil, A.V. and Koli, P.B., 2020. The binary oxide NiO-CuO nanocomposite based thick film sensor for the acute detection of Hydrogen Sulphide gas vapours. *Material Science Research India*, *17*(3), pp.260-269.
23. Xu, S., Yao, Z., Zhou, J. and Du, M., 2018. Effects of post-deposition annealing on the chemical composition, microstructure, optical and mechanical properties of Y2O3 film. *Surface and Coatings Technology*, *344*, pp.636-643.